DESIGN AND ANALYSIS OF DC–DC CONVERTER WITH STEP UP MODE OF BLDC MOTOR

[1]DOLA.RAMU, [2]SRIKANTH REDDIPALLI
[1]M.Tech, Baba Institute of Technology and Sciences under Jawaharlal Nehru Technological University, Kakinada, Andhra Pradesh, India.
[2]Assitant professor, Baba Institute of Technology and Sciences under Jawaharlal Nehru Technological University, Kakinada, Andhra Pradesh, India.

Abstract: In this paper we are implementing a DC-DC converter with the brushless Dc motor. Therefore the circuit configuration of the proposed converter is very simple. in this proposed converter we are analysis an coupled inductor with same winding turns in both the primary and secondary sides. During the step-up mode of operation in parallel charge and series discharge will achieve the high voltage gain. Brushless DC motor is one of the most interesting motor. Not only that it have great efficiency and torque characteristics. Therefore here the proposed converter have higher step up gain comparing with the conventional converter. After comparing the proposed converter and conventional boost converter with same specifications then the average value of the proposed converter is less than the conventional boost converter .The operating principle, torque and speed are verified by the simulation.
Key words: Dc-Dc converter, BLDC motor.

INTRODUCTION

According to the DC–DC converters which is used to transfer the power between two dc sources in either direction. Therefore this converters are widely used in applications, such case like hybrid electric vehicle energy systems [1], uninterrupted power supplies [5], [6], fuel-cell hybrid power systems [7], photovoltaic hybrid power systems and battery chargers.

In recent years, the boost converter is applicable to produce high conversion ratio. But in practical consideration, it is not possible to achieve a high conversion ratio without using a large duty cycle. Due to larger duty ratio and higher components rating, the series problems like reverse recovery, voltage stress and electromagnetic interference will occurs [7-8].In order to avoid the reverse recovery problem, the better solution to use a transformer or coupled inductor [9]. The transformer has a certain limitations like magnetizing and leakage inductances. So, the coupled inductor is simple and better to reduce the conduction loss and current ripple. The secondary side of the coupled inductor will be act as fly back converter, because the capacitor voltage is adjusted by varying the turn ratio. It also degrades the efficiency. the switched capacitor technique was introduced [11]. So, the capacitor can charge in parallel and discharge in series.

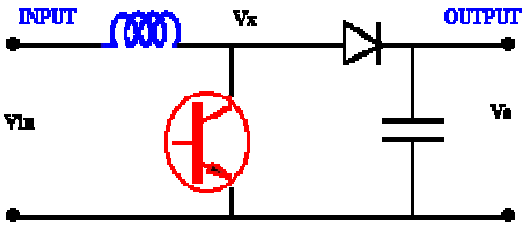

Fig. 1. Conventional dc–dc boost converter

Fig. 1 shows the conventional dc–dc boost converter which is simple structure and easy control. However, the step-up voltage gains are low.

BLDC has excellent efficiency, higher power density and simple control scheme. Controllers that direct the rotation of the rotor is much needed by the motor. Commonly, Hall Effect Sensor or an encoder is used which directly measures the rotor position. Another method is to measure the back emf in the nonmoving coils or known as a sensorless controller. The classical control of BLDC motor basically consists of two power converter; rectifier and three phase PWM inverter. The PWM inverter controlled the current that passed through the motor to maintain the torque and speed at desired value. However, in the classical method, the control loop only involved the PWM inverter while the rectifier is not controlled thus, distorting the current waveform in which the total harmonic distortion is higher [2].

According to the modified dc–dc boost converter which is presented .The voltage gain of this converter is higher than the conventional dc–dc boost converter. The proposed converter employs a coupled inductor with same winding turns in the primary and secondary sides. When comparing with the proposed converter and the conventional bidirectional boost converter, the proposed converter has the following advantages:

1) Higher step-up voltage gains and
2) Lower average value of the switch current under same electric specifications.

The following sections will describe the operating principles and steady-state analysis for the step-up modes. To reduce the voltage stress on the power switch, the low voltage rating switch Rds (ON) will be selected. Due to this selection, the voltage spike across the switch is reduced

significantly. By cascading the boost converter with fly back converter in series, it also improves the voltage gain. By using the concept of coupled inductor and switched capacitor technique the voltage gain is achieved and it also consists of low conduction loss, voltage stress and input current ripple.

STEP-UP MODE

The proposed converter in step-up mode is shown in Fig. 2. The pulsewidth modulation (PWM) technique is used to control the switches S1 and S2 simultaneously.

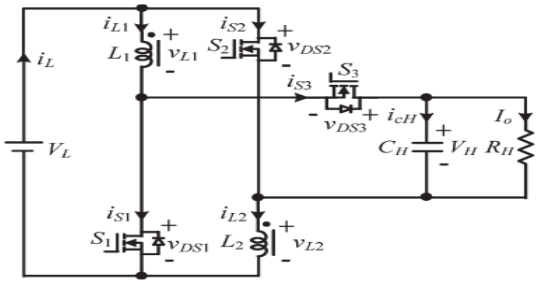

Fig. 2. Proposed converter in step-up mode

The switch S3 is the synchronous rectifier. Since the primary and secondary winding turns of the coupled inductor is same, the inductance of the coupled inductor in the primary and secondary sides are expressed as

$$L_1 = L_2 = L \quad (1)$$

Thus, the mutual inductance M of the coupled inductor is given by

$$M = K\sqrt{L_1 L_2} = kL \quad (2)$$

where k is the coupling coefficient of the coupled inductor. The voltages across the primary and secondary windings of the coupled inductor are as follows:

$$v_{L1} = L_1 \frac{di_{L1}}{dt} + M\frac{di_{L2}}{dt} = L\frac{di_{L1}}{dt} + kL\frac{di_{L2}}{dt} \quad (3)$$

$$v_{L2} = M\frac{di_{L1}}{dt} + L2\frac{di_{L2}}{dt} = kL\frac{di_{L1}}{dt} + L\frac{di_{L2}}{dt} \quad (4)$$

Fig. 3 shows some typical waveforms in continuous conduction mode (CCM) and discontinuous conduction mode (DCM).

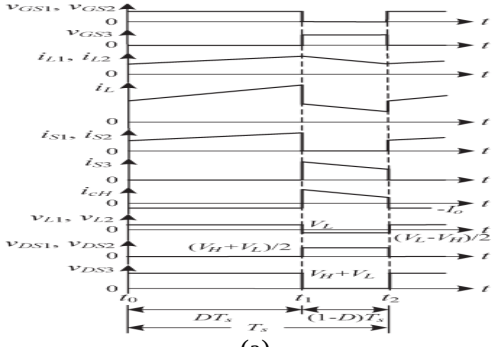

(a)

Fig. 3. Some typical waveforms of the proposed converter in step-up mode. (a) CCM operation

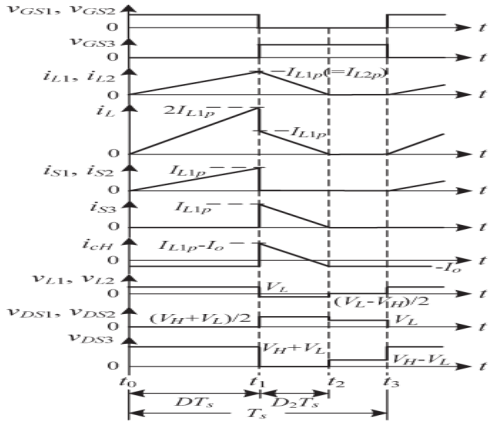

(b)

Fig. 3. Some typical waveforms of the proposed converter in step-up mode. (b) DCM operation.

The operating principles and steady-state analysis of CCM and DCM are described as follows.

A. CCM Operation

1) Mode 1: During this time interval [t0,t1], S1 and S2 are turned on and S3 is turned off. The current flow path is shown in Fig. 4(a).

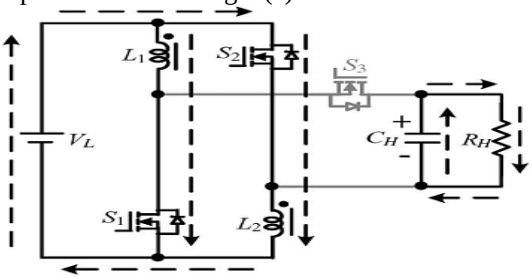

(a)

Fig. 4. Current flow path of the proposed converter in step-up mode. (a) Mode 1.

The energy of the low-voltage side VL is transferred to the coupled inductor. Meanwhile, the primary and secondary windings of the coupled inductor are in parallel. Thus, the voltages across L1 and L2 are obtained as

$$v_{L1} = v_{L2} = V_L \quad (5)$$

Substituting (3) and (4) into (5), yielding

$$\frac{di_{L1}(t)}{dt} = \frac{di_{L2}(t)}{dt} = \frac{V_L}{(1+k)L}, t_0 \le t \le t_1 \quad (6)$$

2) Mode 2: During this time interval [t1,t2], S1 and S2 are turned off and S3 is turned on. The current flow path is shown in Fig. 4(b).

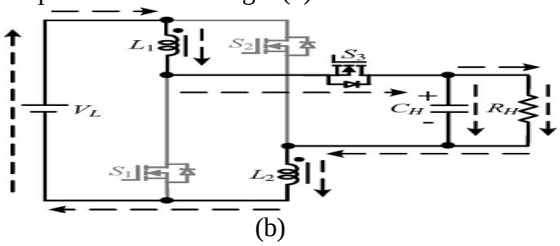

(b)

Fig. 4. Current flow path of the proposed converter in step-up mode. (b) Mode 2

The low-voltage side VL and the coupled inductor are in series to transfer their energies to the capacitor CH and the load. Meanwhile, the primary and secondary windings of the coupled inductor are in series. Thus, the following equations are found to by

$$i_{L1} = i_{L2} \quad (7)$$

$$v_{L1} + v_{L2} = V_L - V_H \quad (8)$$

Substituting (3), (4), and (7) into (8), yielding

$$\frac{di_{L1}(t)}{dt} = \frac{di_{L2}(t)}{dt} = \frac{V_L - V_H}{2(1+k)L}, t_1 \le t \le t_2 \quad (9)$$

By using the state-space averaging method, the following equation is derived from (6) and (9):

$$\frac{DV_L}{(1+k)L} + \frac{(1-D)(V_L - V_H)}{2(1+k)L} = 0 \quad (10)$$

Simplifying (10), the voltage gain is given as

$$G_{CCM(step-up)} = \frac{V_H}{V_L} = \frac{1+D}{1-D} \quad (11)$$

B. DCM Operation

1) Mode 1: During this time interval [t0,t1], S1 and S2 are turned on and S3 is turned off. The current flow path is shown in Fig. 4(a). The operating principle is same as that for the mode 1 of CCM operation. From (6), the two peak currents through the primary and secondary windings of the coupled inductor are given by

$$I_{L1_P} = I_{L2_P} = \frac{V_L D T_S}{(1+k)L} \quad (12)$$

2) Mode 2: During this time interval [t1,t2], S1 and S2 are turned off and S3 is turned on. The current flow path is shown in Fig. 4(b). The low-voltage side VL and the coupled inductor are in series to transfer their energies to the capacitor CH and the load. Meanwhile, the primary and secondary windings of the coupled inductor are in series. The currents iL1 and iL2 through the primary and secondary windings of the coupled inductor are decreased to zero at t = t2. From (9), another expression of IL1p and IL2p is given by

$$I_{L1_P} = I_{L2_P} = \frac{(V_L - V_H) D_2 T_S}{2(1+k)L} \quad (13)$$

3) Mode 3: During this time interval [t2,t3], S1 and S2 are still turned off and S3 is still turned on. The current flow path is shown in Fig. 4(c).

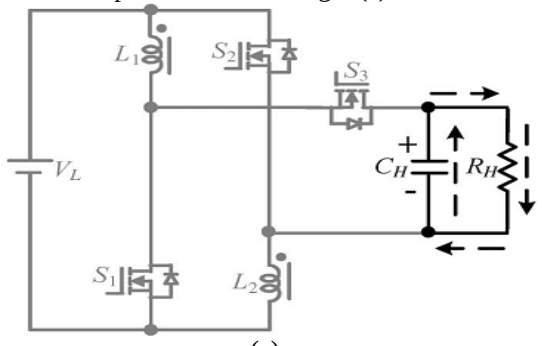

(c)

Fig. 4. Current flow path of the proposed converter in step-up mode. (c) Mode 3 for DCM operation.

The energy stored in the coupled inductor is zero. Thus, iL1 and iL2 are equal to zero. The energy stored in the capacitor CH is discharged to the load. From (12) and (13), D2 is derived as follows:

$$D_2 = \frac{2DV_L}{V_L - V_H} \quad (14)$$

From Fig. 4(b), the average value of the output capacitor current during each switching period is given by

$$I_{CH} = \frac{\frac{1}{2} D_2 T_S I_{L1_P} - I_0 T_S}{T_S} = \frac{1}{2} D_2 I_{L1_P} - I_0 \quad (15)$$

Substituting (12) and (14) into (15), IcH is derived as

$$I_{CH} = \frac{D^2 V_L^2 T_S}{(1+k)L(V_L - V_H)} - \frac{V_H}{R_H} \quad (16)$$

Since IcH is equal to zero under steady state, (16) can be rewritten as follows:

$$\frac{D^2 V_L^2 T_S}{(1+k)L(V_L - V_H)} = \frac{V_H}{R_H} \quad (17)$$

Then, the normalized inductor time constant is defined as

$$T_{LH} = \frac{L}{R_H T_S} = \frac{L f_S}{R_H} \quad (18)$$

where fs is the switching frequency.

Substituting (18) into (17), the voltage gain is given by

$$G_{CCM(step-up)} = \frac{V_H}{V_L} = \frac{1}{2} + \sqrt{\frac{1}{4} + \frac{D^2}{(1+k)\tau_{LH}}} \quad (19)$$

C. Boundary Operating Condition of CCM and DCM

When the proposed converter in step-up mode is operated in boundary conduction mode (BCM), the voltage gain of CCM operation is equal to the voltage gain of DCM operation. From (11) and (19), the boundary normalized inductor time constant τLH,B can be derived as follows:

$$\tau_{LH,B} = \frac{D(1-D)^2}{2(1+k)(1+D)} \quad (20)$$

The curve of τ LH,B is plotted in Fig. 5. If τLH is larger than τLH,B, the proposed converter in step-up mode is operated in CCM.

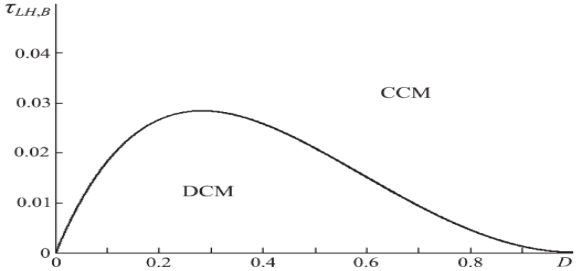

Fig. 5. Boundary condition of the proposed converter in step-up mode (assuming k=1)

COMPARISON OF THE PROPOSED CONVERTER AND CONVENTIONAL BOOST CONVERTER

A. Voltage Gain

The curves of the voltage gain of the proposed converter and conventional bidirectional

boost converter in CCM operation are plotted in Fig. 6. It is seen that the step-up voltage gains of the proposed converter are higher than the conventional boost converter.

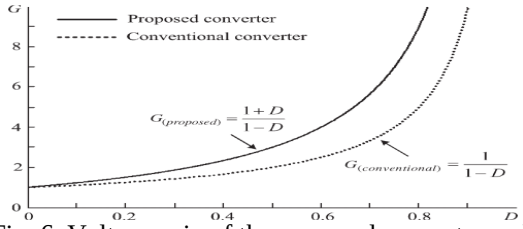

Fig. 6 Voltage gain of the proposed converter and conventional boost in CCM operation Voltage Stress on the Switches

From the voltage stresses on S1, S2, and S3 in the proposed converter are derived as

$$\begin{cases} V_{DS1} = V_{DS2} = \frac{V_H + V_L}{2} \\ V_{DS3} = V_H + V_L \end{cases} \quad (21)$$

As to the voltage stresses on S1 and S2 in the conventional boost converter are given as

$$V_{DS1} = V_{DS2} = V_H \quad (22)$$

Therefore, if the proposed converter is used for high step-up voltage-gain application, the rated voltage of S1 and S2 in the proposed converter can be selected to be lower than the conventional converter. Also, the rated voltage of S3 in the proposed converter can be selected as same as the conventional converter.

B. Average Value of the Switch-Current

When the proposed converter in step-up mode is operated in CCM, the average value of the input current iL is found from Fig.

$$I_{L(proposed)} = \frac{2I_{L1(proposed)}DT_S + I_{L1(proposed)}(1-D)T_S}{T_S} = (1+D)I_{L1(proposed)} \quad (23)$$

where IL1 is the average value of iL1. When the conventional bidirectional boost/buck converter in step-up mode is also operated in CCM, the average value of the input current iL is given by

$$I_{L(conventional)} = I_{L1(conventional)} \quad (24)$$

Under same electric specifications for the proposed converter and conventional bidirectional boost/buck converter, the input power can be expressed as

$$P_{in} = V_L I_{L(conventional)} = V_L I_{L(proposed)} \quad (25)$$

Substituting (23) and (24) into (25), yielding

$$I_{L(proposed)} = \frac{I_{L1(conventional)}}{1+D} \quad (26)$$

When the proposed converter in step-down mode is operated in CCM, the average value of the current iLL is found from Fig. 6(a)

$$I_{LL(proposed)} = \frac{I_{L1(proposed)} + 2I_{L1(proposed)}(1-D)T_S}{T_S} = (2-D)I_{L1(proposed)} \quad (27)$$

Under same electric specifications for the proposed converter and conventional bidirectional boost/buck converter, the output power can be obtained as

$$P_O = V_L I_{L1(conventional)} = V_L I_{LL(proposed)} \quad (28)$$

From (26) and (27), the following equation is derived as:

$$I_{L1(proposed)} = \frac{I_{L1(conventional)}}{2-D} \quad (29)$$

From (25) and (29), one can know that the average value of the switch current in the proposed converter is less than the conventional bidirectional boost/buck converter.

C. Efficiency Analysis

For the proposed converter, the equivalent circuits in step-up mode are shown in Fig. 7. rL1 and rL2 represent the equivalent series resistor (ESR) of the primary and secondary windings of the coupled inductor. rS1, rS2, and rS3 denote the ON-state resistance of S1, S2, and S3, respectively.

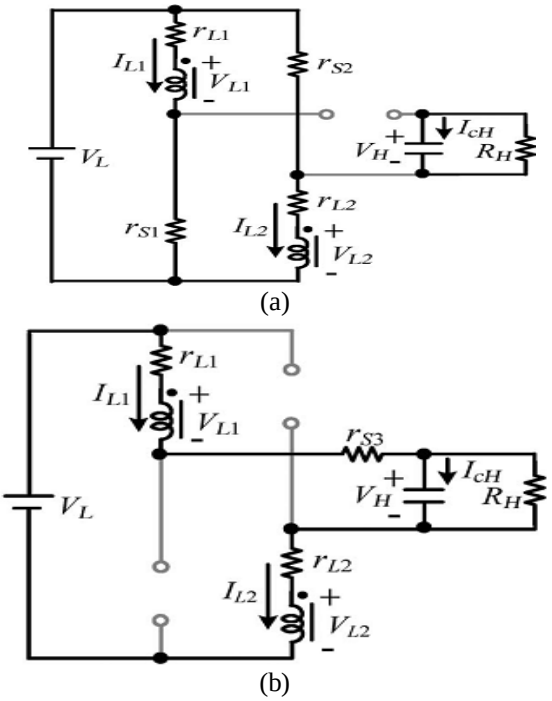

Fig. 7. Equivalent circuit of the proposed converter in step-up mode. (a)S1/S2 ONandS3 OFF.(b)S1/S2 OFFandS3 ON.

When S1/S2 are turned on and S3 is turned off, the equivalent circuit is shown in Fig. 7(a). The average values of icH and vL1 are obtained as

$$I_{cH}^{I} = -\frac{V_H}{R_H} \quad (30)$$

$$V_{L1}^{I} = V_L - I_{L1(r_{L1}+r_{S1})} \quad (31)$$

When S1/S2 are turned off and S3 is turned on, the equivalent circuit is shown in Fig. 7(b). The average values of icH and vL1 are derived as

$$I_{cH}^{II} = I_{L1} - \frac{V_H}{R_H} \quad (32)$$

$$V_{L1}^{II} = \frac{V_L - V_H - I_{L1}(r_{L1}+r_{S3}+r_{L2})}{2} \quad (33)$$

By using the ampere-second balance principle on CH, the following equations are obtained as:

$$\int_0^{DT_S} I_{cH}^{I} dt + \int_0^{(1-D)T_S} I_{cH}^{II} dt = 0 \quad (34)$$

Substituting (27) and (31) into (35), IL1 is given by

$$I_{L1} = \frac{V_H}{(1-D)R_H} \quad (35)$$

Using the volt-second balance principle on L1 yields

$$\int_0^{DT_S} V_{L1}^{I} dt + \int_0^{(1-D)T_S} V_{L1}^{II} dt = 0 \quad (36)$$

Substituting (32) and (34) into (36), the actual voltage gain is derived as

$$\frac{V_H}{V_L} = \frac{1+D}{1-D} \cdot \frac{(1-D)^2 R_H}{(1-D)^2 R_H + 2D(r_{L1}+r_{S1}) + (1-D)(r_{L1}+r_{S3}+r_{L2})} \quad (37)$$

The input power and output power are obtained as

$$P_{in} = 2V_L I_{L1} D + V_L I_{L1}(1-D) = \frac{(1+D)V_L V_H}{(1-D)R_H} \quad (38)$$

$$P_0 = \frac{V_H^2}{R_H} \quad (39)$$

From (37)–(39), the efficiency is found to be

$$\eta = \frac{P_0}{P_{in}} = \frac{(1-D)^2 R_H}{(1-D)^2 R_H + 2D(r_{L1}+r_{S1}) + (1-D)(r_{L1}+r_{S3}+r_{L2})} \quad (40)$$

For the conventional converter, the equivalent circuits in step-up mode are shown in Fig. 14.rL1represents the ESR of the inductor.rS1andrS2 denote ON-state resistance ofS1andS2.

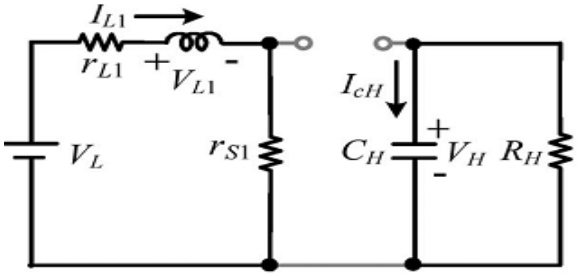

(a)

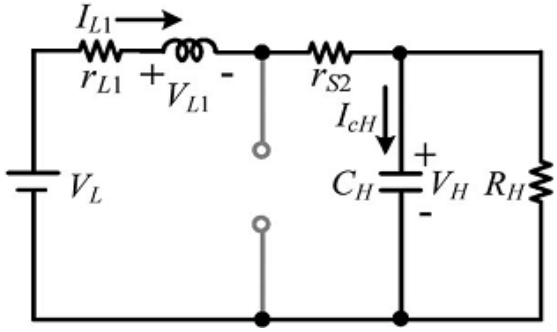

(b)

Fig. 8. Equivalent circuit of the conventional converter in step-up mode. (a)S1ONandS2OFF.(b)S1OFFandS2ON.

According to the foregoing method, the efficiency is derived as follows:

$$\eta = \frac{P_0}{P_{in}} = \frac{(1-D)^2 R_H}{(1-D)^2 R_H + D(r_{L1}+r_{S1}) + (1-D)(r_{L1}+r_{S2})} \quad (41)$$

In order to compare the calculated efficiency for the proposed converter and the conventional converter, some parameters of three cases are assumed as follows:

1) Case 1: rL1=rL2=11mΩ, rS1=rS2=rS3= 23mΩ,VH=42V, and VL=21V.
2) Case 2: rL1=rL2=11mΩ, rS1=rS2=rS3= 23mΩ,VH=42V, and VL=14V.
3) Case 3: rL1=rL2=11mΩ, rS1=rS2=rS3= 23mΩ,VH=42V, and VL=10.5V.

Substituting these parameters the calculated efficiencies of the proposed and conventional converters in step-up modes are shown in Figs. 8 respectively.

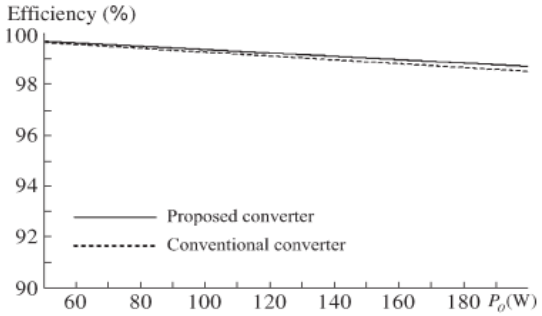

(a)

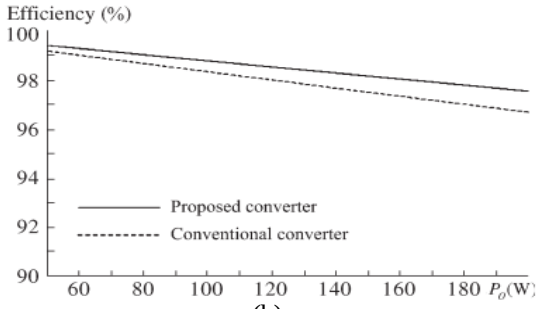

(b)

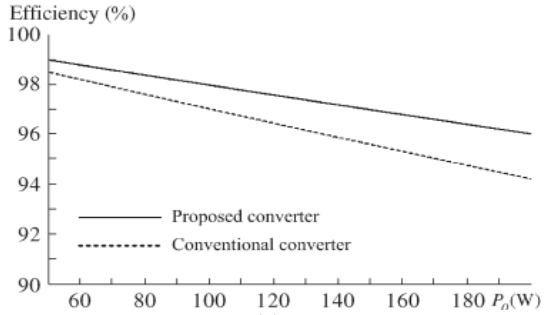

(c)

Fig. 8. Calculated efficiency of the proposed and conventional converters in step-up mode. (a) Case 1. (b) Case 2. (c) Case 3

Thus, if the lower voltage gain is required, the conventional converter can be selected for lower cost. If the higher voltage gain is required, the proposed converter can be chosen for higher efficiency.

PRINCIPLE OF BLDC MOTOR

BLDC engine comprises of the perpetual magnet rotor and an injury stator. The brushless engines are controlled utilizing a three stage inverter. The engine obliges a rotor position sensor for beginning and for giving legitimate compensation arrangement to turn on the force gadgets in the inverter extension. The electronic compensation takes out the issues connected with the brush and the commutator plan, in particular starting and destroying of the commutator brush course of action, along these lines, making a BLDC engine more rough contrasted with a dc engine.

The brush less dc engine comprise of four fundamental parts Power converter, changeless magnet brushless DC Motor (BLDCM), sensors and control calculation. The force converter changes power from the source to the BLDCM which thus changes over electrical vitality to mechanical vitality. One of the remarkable highlights of the brush less dc engine is the rotor position sensors, in view of the rotor position and order signals which may be a torque charge, voltage summon, rate order etc; the control calculation s focus the entryway sign to every semiconductor in the force electronic converter.

The structure of the control calculations decides the sort of the brush less dc engine of which there are two principle classes voltage source based drives and current source based drives. Both voltage source and current source based commute utilized for perpetual magnet brushless DC machine. The back emf waveform of the engine is demonstrated in the fig.10. Be that as it may, machine with a nonsinusoidal back emf brings about diminishment in the inverter size and lessens misfortunes for the same influence level.

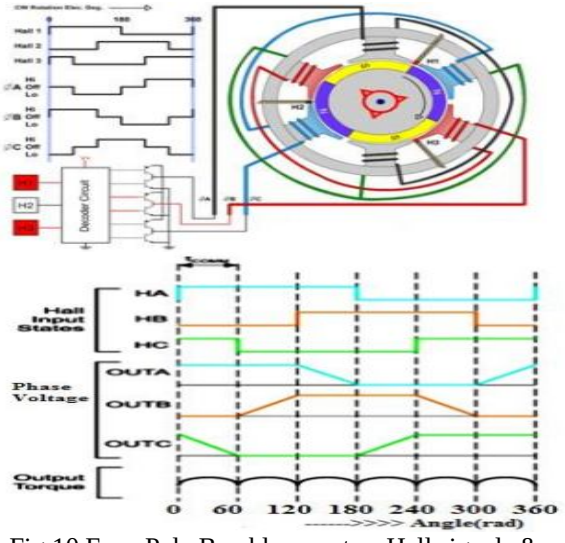

Fig.10.Four-Pole Brushless motor, Hall signals & Stator voltages Commutation, drive and winding timings

SIMULATION RESULT

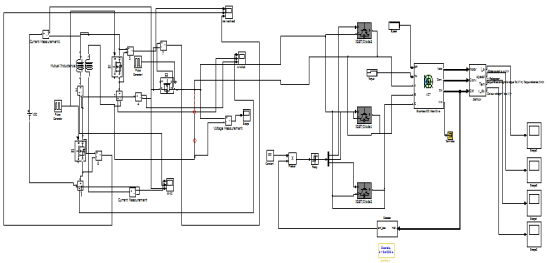

Fig :11 Simulation block diagram of step up BLDC motor

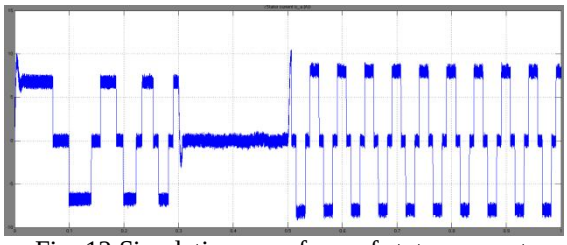

Fig :12 Simulation waveform of stator current

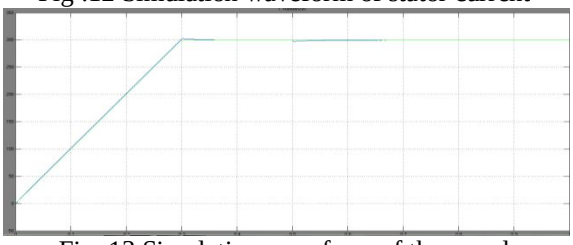

Fig :13 Simulation waveform of the speed

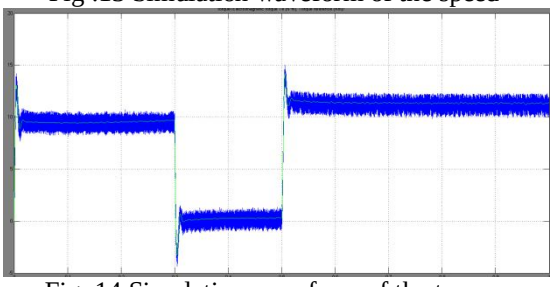

Fig :14 Simulation waveform of the torque

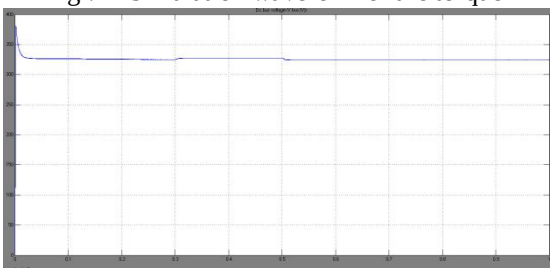

Fig :15 Simulation waveform of DC bus voltage

CONCLUSION

In this paper we are implementing a Dc-Dc converter with the BLDC motor . it is easy to analysis the circuit configuration of the proposed system .therefore the proposed system of Dc- Dc converter have the higher step-up voltage gain and lower value of switch current than the conventional boost converter . Brushless DC motor is one of the most

interesting motor. Not only that it have great efficiency and torque characteristics. Advantages of brushless motors include long life span, little or no maintenance, and high efficiency. From the simulation results, we can analysis the operating principle and steady state analysis of the system. During the full-load condition, the measured efficiency is 92.7% in step-up mode. And also the measured efficiency will be around the 92.7%–96.2% in step-up mode which is higher than the conventional boost converter.

REFERENCES

[1] M. B. Camara, H. Gualous, F. Gustin, A. Berthon, and B. Dakyo, "DC/DC converter design for supercapacitor and battery power management in hybrid vehicle applications—Polynomial control strategy,"IEEE Trans. Ind. Electron., vol. 57, no. 2, pp. 587–597, Feb. 2010.

[2] T. Bhattacharya, V. S. Giri, K. Mathew, and L. Umanand, "Multiphase bidirectional flyback converter topology for hybrid electric vehicles," IEEE Trans. Ind. Electron., vol. 56, no. 1, pp. 78–84, Jan. 2009.

[3] Z. Amjadi and S. S. Williamson, "A novel control technique for a switched-capacitor-converter-based hybrid electric vehicle energy storage system,"IEEE Trans. Ind. Electron., vol. 57, no. 3, pp. 926–934, Mar. 2010.

[4] F. Z. Peng, F. Zhang, and Z. Qian, "A magnetic-less dc–dc converter for dual-voltage automotive systems,"IEEE Trans. Ind. Appl., vol. 39, no. 2, pp. 511–518, Mar./Apr. 2003.

[5] A. Nasiri, Z. Nie, S. B. Bekiarov, and A. Emadi, "An on-line UPS system with power factor correction and electric isolation using BIFRED converter,"IEEE Trans. Ind. Electron., vol. 55, no. 2, pp. 722–730, Feb. 2008.

[6] L. Schuch, C. Rech, H. L. Hey, H. A. Grundling, H. Pinheiro, and J. R. Pinheiro, "Analysis and design of a new high-efficiency bidirectional integrated ZVT PWM converter for DC-bus and battery-bank interface," IEEE Trans. Ind. Appl., vol. 42, no. 5, pp. 1321–1332, Sep./Oct. 2006.

[7] X. Zhu, X. Li, G. Shen, and D. Xu, "Design of the dynamic power compensation for PEMFC distributed power system,"IEEE Trans. Ind. Electron., vol. 57, no. 6, pp. 1935–1944, Jun. 2010.

[8] G. Ma, W. Qu, G. Yu, Y. Liu, N. Liang, and W. Li, "A zero-voltageswitching bidirectional dc–dc converter with state analysis and softswitching-oriented design consideration," IEEE Trans. Ind. Electron., vol. 56, no. 6, pp. 2174–2184, Jun. 2009.

[9] F. Z. Peng, H. Li, G. J. Su, and J. S. Lawler, "A new ZVS bidirectional dc–dc converter for fuel cell and battery application,"IEEE Trans. Power Electron., vol. 19, no. 1, pp. 54–65, Jan. 2004.

DOLA RAMU

Completed B.Tech in Electrical & Electronics Engineering in2012 from JNTUUNIVERSITY, KAKINADA and Pursuing M.Tech from Baba Institute of Technology and Sciences Affiliated to JNTUK, Kakinada, Madhurawada, Visakhapatnam, and Andhra Pradesh, India. Area of interest includes Power Electronics**.**
E-mail id **: dolaramu.eee@gmail.com**

SRIKANTH REDDIPALLI

Completed B.Tech in Electrical &Electronics Engineering in 2008 from Sriprakash College of Engineering Tuni, and M.Tech in Electrical Power Systems &Automation in 2011from GITAM University, Visakhapatnam. Currently working as Assistant Professor at Baba Institute of Technology and Sciences Affiliated to JNTUK, Kakinada, Madhurawada, Visakhapatnam, Andhra Pradesh, India. Area of interest includes **Power Quality, Electrical Drives and Machines.**
E-mail id: **srikanthreddipalli@gmail.com**